The Plant Cell, Vol. 26: 2889–2904, July 2014, www.plantcell.org

TAA1-Regulated Local Auxin Biosynthesis in the Root-Apex Transition Zone Mediates the Aluminum-Induced Inhibition of Root Growth in *Arabidopsis*[C][W][OPEN]

Zhong-Bao Yang,[a] Xiaoyu Geng,[a] Chunmei He,[a] Feng Zhang,[a] Rong Wang,[a] Walter J. Horst,[b] and Zhaojun Ding[a,1]

[a] Key Laboratory of Plant Cell Engineering and Germplasm Innovation, Ministry of Education, College of Life Science, Shandong University, Jinan 250100, People's Republic of China

[b] Institute of Plant Nutrition, Leibniz Universität Hannover, 30419 Hannover, Germany

The transition zone (TZ) of the root apex is the perception site of Al toxicity. Here, we show that exposure of *Arabidopsis thaliana* roots to Al induces a localized enhancement of auxin signaling in the root-apex TZ that is dependent on *TAA1*, which encodes a Trp aminotransferase and regulates auxin biosynthesis. *TAA1* is specifically upregulated in the root-apex TZ in response to Al treatment, thus mediating local auxin biosynthesis and inhibition of root growth. The TAA1-regulated local auxin biosynthesis in the root-apex TZ in response to Al stress is dependent on ethylene, as revealed by manipulating ethylene homeostasis via the precursor of ethylene biosynthesis 1-aminocyclopropane-1-carboxylic acid, the inhibitor of ethylene biosynthesis aminoethoxyvinylglycine, or mutant analysis. In response to Al stress, ethylene signaling locally upregulates *TAA1* expression and thus auxin responses in the TZ and results in auxin-regulated root growth inhibition through a number of auxin response factors (ARFs). In particular, ARF10 and ARF16 are important in the regulation of cell wall modification–related genes. Our study suggests a mechanism underlying how environmental cues affect root growth plasticity through influencing local auxin biosynthesis and signaling.

INTRODUCTION

Al is the most abundant metal in the earth's crust. In acidic soils (pH < 5), the phytotoxic Al^{3+} ion becomes increasingly soluble and becomes a significant constraint on crop productivity. Acidic soils are widespread, especially in the tropics and subtropics (Von Uexküll and Mutert, 1995; Kochian et al., 2004). The inhibition of root elongation has been widely used as a bioassay for Al toxicity (Delhaize and Ryan, 1995). The root apex is the major target site of Al toxicity (Ryan and Kochian, 1993); in maize (*Zea mays*), the distal part of the root-apex transition zone (TZ), located between the apical meristem and the basal elongation region, is the most Al-sensitive part of the root (Sivaguru and Horst, 1998), and a similar zone is involved in both common bean (*Phaseolus vulgaris*) (Rangel et al., 2007) and *Arabidopsis thaliana* (Illés et al., 2006). The importance of the distal part of the root TZ in the response to Al toxicity has been confirmed in sorghum (*Sorghum bicolor*) by the demonstration that it is the site of reactive oxygen species production (Sivaguru et al., 2013).

Tissue- or cell-specific hormone signaling is an important component of the regulation of root growth (Gifford et al., 2008; Ding and De Smet, 2013; Duan et al., 2013; Rosquete et al., 2013). The root-apex TZ is a critical site for the perception and response to both endogenous phytohormones and environmental cues (Baluška et al., 2010), particularly to auxin, the key regulator of root development (Benková and Hejátko, 2009; Overvoorde et al., 2010; Bielach et al., 2012; Jansen et al., 2012; Lavenus et al., 2013). In conjunction with auxin, ethylene is also involved in the regulation of root growth (Růzicka et al., 2007; Swarup et al., 2007). Ethylene can regulate auxin biosynthesis and basipetal auxin transport toward the elongation zone, which activates auxin signaling in the root apex, and thus causes root growth inhibition (Růzicka et al., 2007; Stepanova et al., 2007, 2011; Swarup et al., 2007). It was recently reported that ethylene signaling regulates the expression of Trp aminotransferase/Trp aminotransferase–related proteins (TAA1/TARs), which catalyze the key step of auxin biosynthesis through the conversion of Trp to indole-3-pyruvic acid, thus positively directing auxin biosynthesis (Stepanova et al., 2008; He et al., 2011).

Al-regulated inhibition of root growth is clearly regulated by auxin (Kollmeier et al., 2000; Sun et al., 2010). High-throughput sequencing analysis of the Al-regulated microRNAs in wild soybean (*Glycine soja*) (Zeng et al., 2012) and *Medicago truncatula* (Chen et al., 2012) revealed the potential regulation of microRNA160 (miR160) in the Al-induced inhibition of root growth through mediating the expression of auxin response factors (ARFs) such as *ARF10* and *ARF16* (Wang et al., 2005; Liu et al., 2007; Liu et al., 2010). The targeted application of Al to the distal part of the root-apex TZ has been shown to be as inhibitory as when it is applied over the entire maize root apex (Sivaguru et al., 1999; Kollmeier et al., 2000), while the localized application of Al to the root-apex elongation zone (EZ) has little effect on root elongation. The implication is that signaling between the root-apex TZ and EZ determines the extent of Al-induced inhibition of root growth. The

[1] Address correspondence to dingzhaojun@sdu.edu.cn.
The author responsible for distribution of materials integral to the findings presented in this article in accordance with the policy described in the Instructions for Authors (www.plantcell.org) is: Zhaojun Ding (dingzhaojun@sdu.edu.cn).

[C] Some figures in this article are displayed in color online but in black and white in the print edition.

[W] Online version contains Web-only data.

[OPEN] Articles can be viewed online without a subscription.

www.plantcell.org/cgi/doi/10.1105/tpc.114.127993

exogenous supply of the auxin indole-3-acetic acid (IAA) to the EZ significantly reduces the extent of Al-induced root elongation inhibition, but the same treatment given to the meristematic zone has no effect (Kollmeier et al., 2000). The presence of Al promotes the accumulation of auxin in the root cap, the root apical meristem, and the distal part of the TZ (Kollmeier et al., 2000; Sun et al., 2010) as a result of the disruption caused to auxin transport from the distal part of the root-apex TZ to the EZ (Sivaguru et al., 1999; Kollmeier et al., 2000; Doncheva et al., 2005). Since an elevated level of auxin in the EZ is required for cell elongation (Teale et al., 2005, 2006), it is probable that the regulation of Al-induced root growth involves the inhibition of basipetal auxin transport, mediated by auxin signaling between the TZ and EZ (Kollmeier et al., 2000).

As yet, how auxin levels in the TZ and EZ mediate the Al-regulated inhibition of root growth remains largely unknown. Here, we exploited a green fluorescent protein (GFP)–tagged auxin-responsive *DR5rev:GFP* transgene, the expression of which provides a robust spatial representation of auxin distribution (Ding and Friml, 2010; Tian et al., 2013, 2014a), to monitor auxin activity in the *Arabidopsis* root-apex TZ as induced by externally applied Al. This tool has allowed us to show that the activity of TAA1 was essential for auxin accumulation in the root-apex TZ in response to Al stress. In addition, our investigations indicate that the local upregulation of TAA1 and the resulting local auxin accumulation in the root-apex TZ constitute an ethylene signaling–dependent process. Moreover, our data also show that auxin plays a negative role in Al stress–regulated root growth via regulating the expression of cell wall modification–related genes in *Arabidopsis*.

RESULTS

The Auxin Signaling Maximum in the Root-Apex TZ Is Crucial for Root Growth Inhibition in Response to Al Stress

The root-apex TZ, as expected from the findings of Sivaguru and Horst (1998) in maize, proved to be the perception site of Al toxicity in *Arabidopsis* as well, as demonstrated by the staining pattern of propidium iodide (PI), which accumulates only in dying and dead cells, and fluorescein diacetate (FDA) staining, which is taken up and converted into the green fluorescent compound "fluorescin" only by living cells (Supplemental Figure 1; Moore et al., 1998; Steward et al., 1999).

The distribution of auxin in the root tip of plants exposed to Al was revealed by employing the auxin-responsive reporter construct *DR5rev:GFP*. After a 2-h exposure to 10 μM Al, an increased DR5 activity was detected specifically in the epidermis and cortex region of the root TZ, and increasing the concentration of Al to 25 μM produced even stronger DR5rev:GFP signals (Figure 1A). Further time-course analysis of DR5rev:GFP signals in the presence of 6 μM Al revealed that the DR5rev:GFP signals in the TZ increased until 12 h and, thereafter, remarkably decreased and even disappeared after 7 d of exposure to toxic Al (Supplemental Figure 2), suggesting that auxin may act as an early Al-responsive signal to regulate the Al-induced root growth inhibition. To test whether the Al-induced auxin reporter DR5rev:GFP signaling maximum in the TZ reflects the endogenous increased auxin level, we measured the concentration of IAA in 1-mm-long root tips (the region including the meristematic, transition, and fast elongation zones according to Verbelen et al., 2006). In agreement with the increased *DR5rev:GFP* expression in the TZ, 6 μM Al significantly increased the endogenous auxin levels in root tips (1 mm from the apex) after 6 and 12 h of Al exposure (Figure 1B). The undetected increment of free IAA levels after 3 h of Al treatment might be due to the small induction of local auxin production only in the TZ, which is masked when analyzing the whole root-tip tissues.

The correlation between auxin response in the root-apex TZ and inhibition of root growth was investigated by exposing seedlings to both Al and the auxin antagonist α-(phenylethyl-2-one)-indole-3-acetic acid (PEO-IAA), a molecule that blocks the auxin binding sites of TIR1/AFB auxin receptors (Hayashi et al., 2008; Nishimura et al., 2009; Hayashi, 2012). The Al treatment–induced DR5rev:GFP signals in the root-apex TZ were markedly reduced by PEO-IAA (Figure 1A), and the effect of increasing the Al supply on root growth was reduced (Figures 1C and 1D; Supplemental Figure 3). These results clearly suggest that the Al-induced auxin response in the root-apex TZ is involved in the Al-induced inhibition of root growth.

Auxin Enhances the Al-Induced Inhibition of Root Growth

To confirm the role of auxin in Al-induced root growth inhibition, further experiments were performed via manipulating auxin levels or auxin signaling through exogenous 1-naphthaleneacetic acid (NAA) application or mutant analysis. A low concentration of Al (≤3 μM) in the growing medium tended to promote rather than to inhibit root elongation. The presence of 2.5 nM NAA had no effect on root growth without Al supply, although the expression of *DR5rev:GFP* increased in the whole root apex particularly in the apical meristem zone after 6 h of NAA exposure (Supplemental Figure 4). However, when the roots were exposed to levels of Al >1 μM, NAA substantially enhanced the extent of Al-induced growth inhibition (Figures 2A and 2B). At 5 μM Al, the effect of NAA on the level of inhibition was even more pronounced (Figure 2C). However, the NAA-enhanced Al-induced root growth inhibition did not result from the specific increase in auxin signaling in the TZ. Instead, the whole root apex showed higher DR5rev:GFP signals, particularly clearly after 12 h of treatment (Supplemental Figure 4). Several auxin-responsive genes, including *IAA7*, *IAA10*, *IAA14*, and *IAA18* (in the AUXIN/IAA gene family), *GH3.2*, *GH3.3*, *GH3.5*, *GH3.12*, and *AT5G13370* (in the GRETCHEN HAGEN3 gene family), and *SAUR37* and *SAUR59* (in the SMALL AUXIN-UP RNA gene family), were selected from the results generated by RNA sequencing (RNAseq) (Supplemental Data Set 1) to check their response to the NAA and/or Al treatments by quantitative real-time PCR (qRT-PCR). The results showed that, independently, NAA or Al treatment significantly induced the expression of most of the selected genes at 6 and 12 h, while combined NAA and Al treatments led to higher gene expression than either NAA or Al treatment alone mainly for the GH3 gene family, including *GH3.2*, *GH3.3*, *GH3.5*, *GH3.12*, and *AT5G13370* (Supplemental Figure 5). This suggests an additive effect of NAA and Al on auxin signaling and the potential regulation of the GH3 gene family in Al-induced root growth inhibition at an early stage.

The gain-of-function *solitary root1* (*slr-1*) mutant, in which a stabilized form of the AUX/IAA14 protein is present, leading to

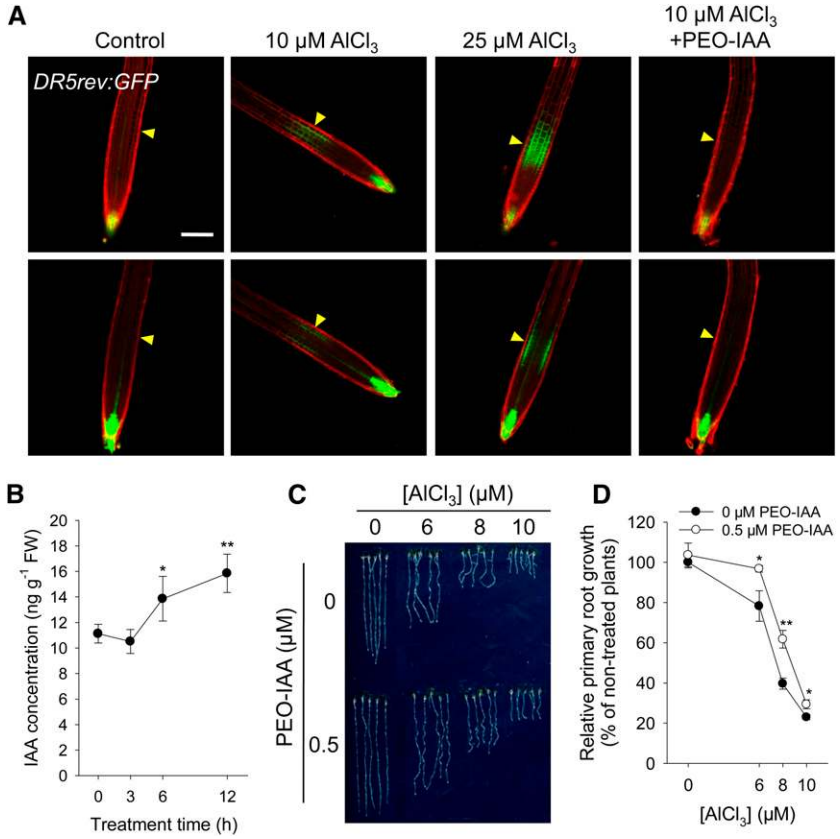

Figure 1. The Al-Induced Auxin Response in the TZ Is Crucial for Root Growth Inhibition in *Arabidopsis*.

(A) Expression of the *DR5rev:GFP* transgene in roots exposed for 2 h to 0, 10, or 25 μM $AlCl_3$ or to 10 μM $AlCl_3$ plus 15 μM PEO-IAA. Control indicates nontreated roots. The top row shows *DR5rev:GFP* signals in the epidermis, and the bottom row shows *DR5rev:GFP* signals in the cortex. Cell boundaries appear red following PI staining. The TZ is marked by yellow arrowheads. Bar = 100 μm.

(B) IAA concentration in root tips (1 mm long) exposed to 6, 8, and 10 μM $AlCl_3$ for 0, 3, 6, and 12 h. Asterisks indicate significant differences at *P < 0.05 and **P < 0.01 (*t* test). Values represent means ± SD (*n* = 3). FW, fresh weight.

(C) and **(D)** Primary root growth after exposure to 0, 6, 8, and 10 μM $AlCl_3$ and either 0 or 0.5 μM PEO-IAA for 7 d. Asterisks indicate that differences between the PEO-IAA treatments are significant at *P < 0.05 and **P < 0.01 (*t* test). Values in **(D)** represent means ± SD (*n* = 30).

a reduced level of auxin signaling (Fukaki et al., 2002), showed a more strongly reduced root growth inhibition in the presence of Al than the wild type (Figure 2D). Both the dominant *Arabidopsis yucca* (*yuc1D*) mutant, which is characterized by a high endogenous IAA level as a result of the overexpression of a rate-limiting auxin synthesis gene (Zhao et al., 2001), and the *pin-formed8* overexpressor (*PIN8 OX*) mutant, which also accumulates higher free IAA in its roots (Ding et al., 2012), exhibited stronger inhibition of root growth in the presence of Al than the wild-type plants (Figures 2E and 2F). These results imply that the elevated levels of free auxin enhance the Al-induced inhibition of root growth.

Both Auxin Signaling Maximum in the TZ and Al-Induced Inhibition of Root Growth Are Regulated by TAA1

To test if auxin biosynthesis is involved in the Al-induced local auxin signaling maximum and root growth inhibition, we first examined the phenotypes of the *TAA1* mutant *taa1-1*, which is defective in the indole-3-pyruvic acid branch of the auxin synthetic pathway and exhibits a reduced auxin level in its roots (Stepanova et al., 2008; Tao et al., 2008). In *taa1-1* root tips, the Al treatment–induced boosting of DR5rev:GFP signals in the TZ shown by the wild type did not occur (Figure 3A). Consistently, the root growth inhibition in the presence of Al stress was also significantly alleviated in *taa1-1* compared with the wild-type controls (Figures 3B and 3C). The small molecule L-kynurenine (Kyn) can effectively and selectively bind to the substrate pocket of TAA1/TAR proteins, and thus competitively inhibit TAA1/TAR activity, mimicking the loss of TAA1/TAR functions (He et al., 2011). Treatment of roots with Kyn only reduced root growth at >1 μM Kyn in the medium in the absence of Al (Figures 3D and 3E). However, when Al was included in the medium, 0.5 or 1 μM Kyn largely alleviated the Al-induced inhibition of root growth (Figures 3D and 3E), suggesting that the TAA1-regulated local auxin biosynthesis mediates the auxin signaling maximum in the root-apex TZ and thus root growth inhibition in response to Al stress.

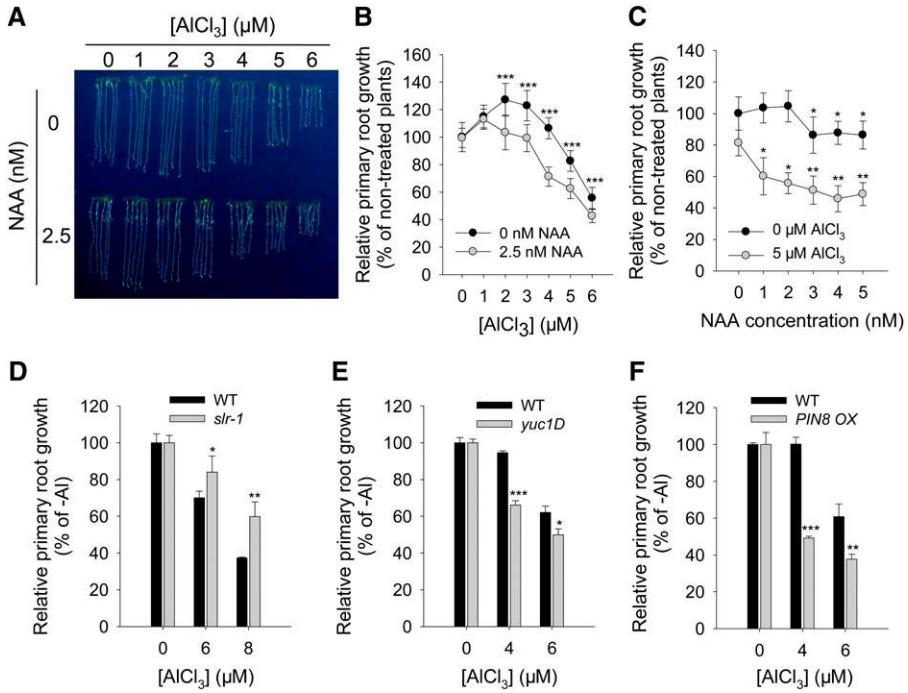

Figure 2. Auxin Mediates the Al-Induced Inhibition of Root Growth.

(A) to **(C)** Effect of exogenous NAA on root growth following a 7-d exposure to 0 or 2.5 nM NAA in the presence of 0 to 6 μM $AlCl_3$ (**[A]** and **[B]**) or 0 to 5 nM NAA in the presence of 0 or 5 μM $AlCl_3$ **(C)**. Asterisks in **(B)** and **(C)** indicate that NAA treatments differ significantly at *P < 0.05, **P < 0.01, and ***P < 0.001 (*t* test).

(D) to **(F)** Root growth after a 7-d exposure to $AlCl_3$. Wild-type plants and gain-of-function mutants *slr-1*, *PIN8 OX*, and *yuc1D* were exposed to 0, 4, 6, or 8 μM $AlCl_3$. Asterisks indicate that means within the wild type and *slr-1*, *PIN8 OX*, or *yuc1D* in each Al concentration differ significantly at *P < 0.05, **P < 0.01, and ***P < 0.001 (*t* test).

Values in **(B)** to **(F)** represent means ± SD (n = 30).

[See online article for color version of this figure.]

TAA1 Is Locally Induced in the TZ by the Presence of Al

To explore how TAA1 regulates local auxin signaling in the TZ of root tips in the presence of Al, the effect of exogenous Al on the spatial expression of *TAA1* was examined using the *TAA1:GFP-TAA1* translational fusion transgene. The transgene is expressed mainly in the root tip, specifically in the zone surrounding the root quiescent center (Stepanova et al., 2008). A clear GFP signal was observed in the TZ after a 2-h exposure to Al (Figure 4). The dynamic expression of Al-induced *TAA1:GFP* at different time points of Al exposure (0 to 48 h and 7 d) was consistent with the changes in DR5rev:GFP signals, showing the highest induction of TAA1 after 12 h of treatment (compare Supplemental Figures 2 and 6). Similar to *DR5rev:GFP*, the local induction of TAA1 in the TZ was also absent on day 7 of Al exposure. This result confirmed the early regulatory role of TAA1 for the local auxin signaling maximum in the root-apex TZ in response to Al stress. However, no expressional change of *TAA1* and its homolog *TARs* at the transcript level was found in Al-exposed whole roots through RNAseq analysis (Supplemental Data Set 1); the potential increase in gene expression in the TZ might be masked when analyzing the whole roots.

Decreasing the pH of the medium from 5.5 to 4.2 reduced the growth of the root severely (Supplemental Figure 7) but did not affect the expression of either the *DR5rev:GFP* or the *TAA1:GFP* transgene (Supplemental Figure 8), implying that exogenous Al, not protons, upregulates *TAA1*, driving up the accumulation of auxin in the TZ and, finally, inhibiting root growth.

Al-Induced Local TAA1 Expression in the TZ Is Regulated by Ethylene

Recently, Stepanova et al. (2008) and He et al. (2011) found that TAA1-mediated auxin biosynthesis in the root apex was regulated by ethylene, and mutations in *TAA1* resulted in root-specific ethylene insensitivity (Stepanova et al., 2008). To study if the Al-induced local TAA1 expression in the TZ is dependent on ethylene signaling, we examined local *TAA1:GFP* induction in response to Al when cotreated with the precursor of ethylene biosynthesis 1-aminocyclopropane-1-carboxylic acid (ACC) or the inhibitor of ethylene biosynthesis aminoethoxyvinylglycine (AVG). The Al-induced local *TAA1:GFP* signals in the TZ were strongly intensified by ACC cotreatment, while they were highly repressed by AVG (Figure 5A). Consistent with these results, application of exogenous ACC or AVG significantly enhanced or alleviated the Al-induced inhibition of primary root growth, respectively (Figures 5B and 5C).

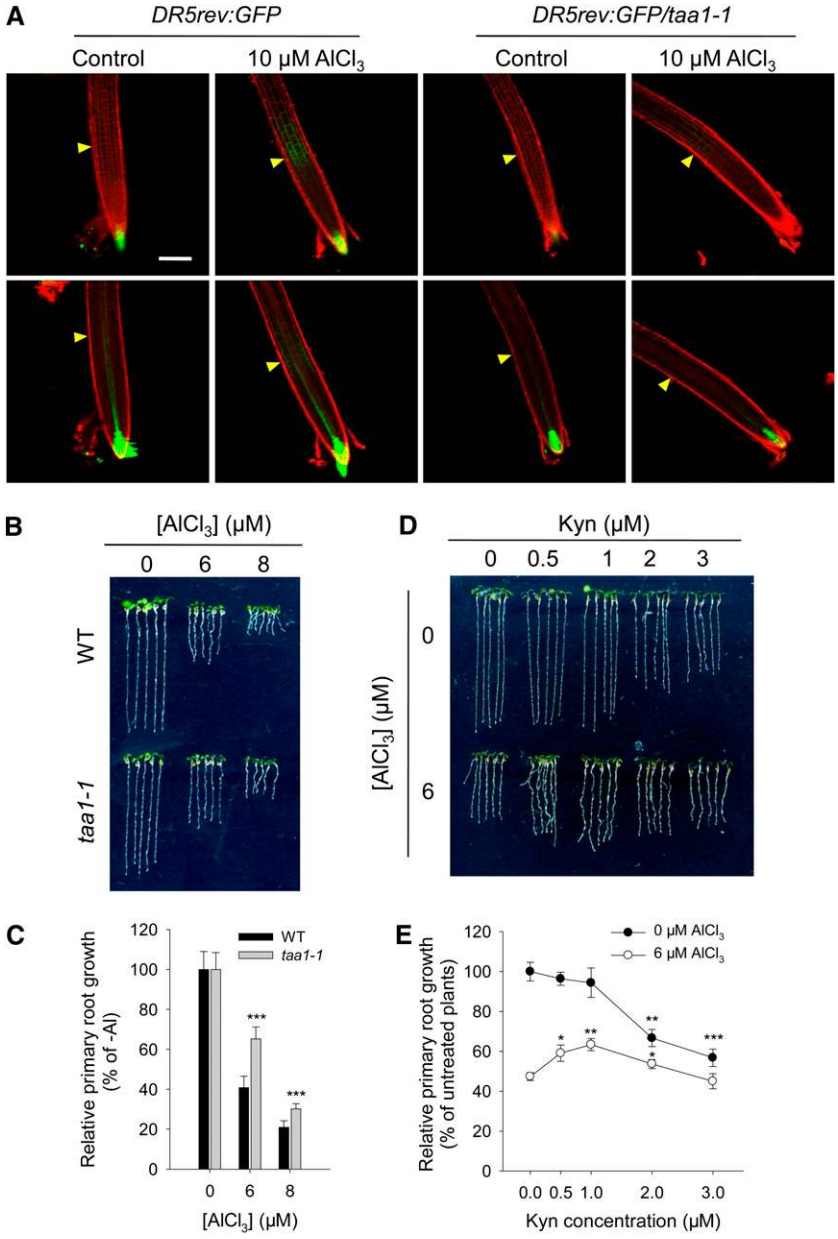

Figure 3. Both Auxin Signaling Maximum in the TZ and Al-Induced Inhibition of Root Growth Are Regulated by TAA1.

(A) Expression of the *DR5rev:GFP* transgene in the root tip of the wild type and the loss-of-function mutant *taa1-1*. Six-day-old *DR5rev:GFP* and *DR5rev:GFP/taa1-1* seedlings were exposed for 2 h to either 0 (control) or 10 μM $AlCl_3$. The top row shows DR5rev:GFP signals in the epidermis, and the bottom row shows DR5rev:GFP signals in the cortex. Cell boundaries appear red following PI staining. The TZ is marked by yellow arrowheads. Bar = 100 μm.

(B) and **(C)** Root growth of wild-type and *taa1-1* plants after a 7-d exposure to 0, 6, or 8 μM $AlCl_3$. Asterisks in **(C)** indicate that means within the wild type and the *taa1-1* mutant in each Al concentration differ significantly at ***$P < 0.001$ (*t* test).

(D) and **(E)** Effect on the Al-induced inhibition of root growth of adding the TAA1 inhibitor Kyn. Root growth was measured after a 7-d exposure to 0 or 6 μM $AlCl_3$ in the presence of 0 to 3 μM Kyn. Asterisks in **(E)** indicate that Kyn treatments differ significantly at *$P < 0.05$, **$P < 0.01$, and ***$P < 0.001$ (*t* test). Values in **(C)** and **(E)** represent means ± SD ($n = 30$).

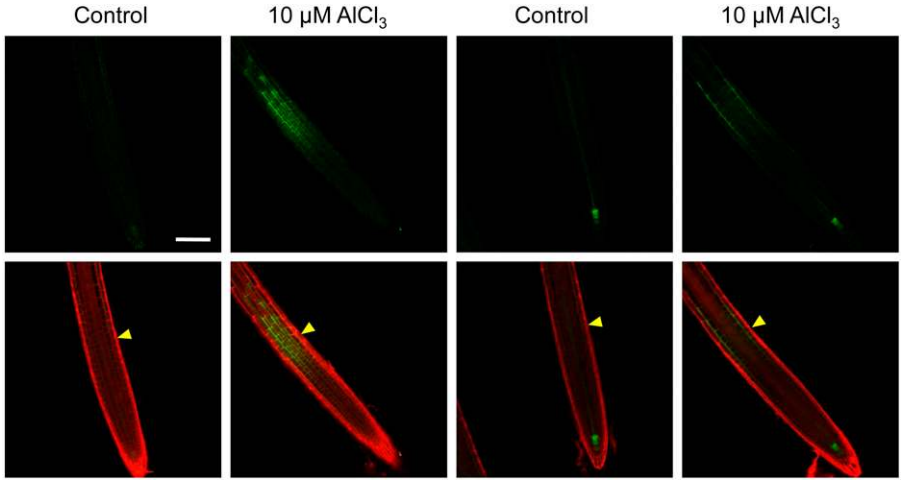

Figure 4. Al Induces *TAA1:GFP* Expression in the TZ.

Six-day-old transgenic *TAA1:GFP* seedlings were exposed to either 0 (control) or 10 μM $AlCl_3$ for 2 h. The two left columns show TAA1:GFP signals in the epidermis, and the two right columns show TAA1:GFP signals in the cortex. The top row shows the expression of *TAA1:GFP*, while the bottom row shows an overlay of the *TAA1:GFP* expression and PI staining (the latter used to highlight cell boundaries). The TZ is marked by yellow arrowheads. Bar = 100 μm.

TAA1-Regulated Local Auxin Response in the TZ and Inhibition of Root Growth in Response to Al Depends on Ethylene Signaling

To identify if ethylene-regulated local *TAA1* upregulation contributes to the local auxin signaling maximum in the TZ and thus to the inhibition of root growth in response to Al exposure, the local DR5rev:GFP signals in the TZ under cotreatment with ACC or AVG with Al were examined. The application of exogenous ACC strongly enhanced DR5rev:GFP signals, while AVG cotreatment highly repressed the local DR5rev:GFP signals in the TZ in response to Al exposure (Figure 6A). However, ACC and ACC plus Al treatment intensified the DR5rev:GFP signals along the whole root apex, indicating that the ACC-enhanced Al-induced root growth inhibition was not due to the specific increase in the auxin response in the TZ (Figure 6A; Supplemental Figure 9).

To address if TAA1-mediated local auxin biosynthesis acts downstream of ethylene signaling in response to Al exposure, the response of *taa1-1* to ACC under Al stress was tested. ACC treatment at up to 50 nM did not affect the root growth of wild-type and *taa1-1* plants (Figure 6B). However, the Al-induced root growth inhibition was significantly enhanced by 50 nM ACC only in the wild type but not in *taa1-1* (Figure 6B). Furthermore, the inhibitor of TAA1/TAR-dependent auxin biosynthesis, Kyn, which slightly reduced the root growth of wild-type plants at 2 μM but not at 1 μM, clearly alleviated at both concentrations the root growth–inhibiting additive effects of 50 nM ACC and 6 μM Al cotreatment (Figure 6C). In order to clarify the possible role of auxin as a downstream signal of ethylene to regulate Al-induced inhibition of root growth, the additive effects of auxin on Al-induced root growth inhibition were studied in *eto1-2* (for ethylene overproducer; He et al., 2011) and the double mutant *ein3-1 eil1-1* (for ethylene insensitive; Alonso et al., 2003). Confirming the role of ethylene, Al-induced root growth inhibition was enhanced in *eto1-2* (Figure 6D) but alleviated in *ein3-1 eil1-1* (Figure 6E) compared with the wild type. However, the application of exogenous NAA (2.5 nM) consistently and significantly enhanced the Al-induced root growth inhibition in both *eto1-2* and *ein3-1 eil1-1* mutants, similar to the wild type (Figures 6D and 6E), implying that auxin acts downstream of ethylene to regulate Al-induced root growth inhibition.

ARFs Are Involved in Al-Induced Inhibition of Root Growth

ARFs are a class of transcription factors involved in the auxin signaling pathway, which is an important component of plant development and growth responses to various environmental stimuli (Guilfoyle and Hagen, 2007; Ding and Friml, 2010; Tian et al., 2014a). To explore the role of auxin signaling in Al-induced root growth inhibition, the response to Al of a set of 24 loss-of-function *ARF* mutants was compared with that of the wild type. The Al-induced inhibition of root growth in the single mutants *arf1*, *arf6*, *arf8*, *arf9*, *arf10*, and *arf16*, and particularly in the double mutants *arf7/19* and *arf10/16*, was less severe than in the wild type (Figure 7A). However, the ARF mutants did not differ in transcript levels in response to Al treatment, according to the results of RNAseq (Supplemental Data Set 1). To understand how ARFs regulate Al-induced root growth inhibition, the *arf10/16* double mutant was selected for further experiments, since particularly high levels of expression of *ARF10* and *ARF16* were observed in the epidermis and cortex of the root apex (Supplemental Figure 10), the major perception site of Al toxicity (Ryan et al., 1993). A dose–response experiment confirmed the marked reduction of Al-induced inhibition of root growth in the *arf10/16* double mutant compared with the wild type (Figures 7B and 7C). A lower intensity of morin staining (which stains Al) in the double mutant root after a 24-h exposure to 10 μM Al (Figure 7D) suggests that its reduced Al sensitivity is due to a lower Al accumulation in the TZ.

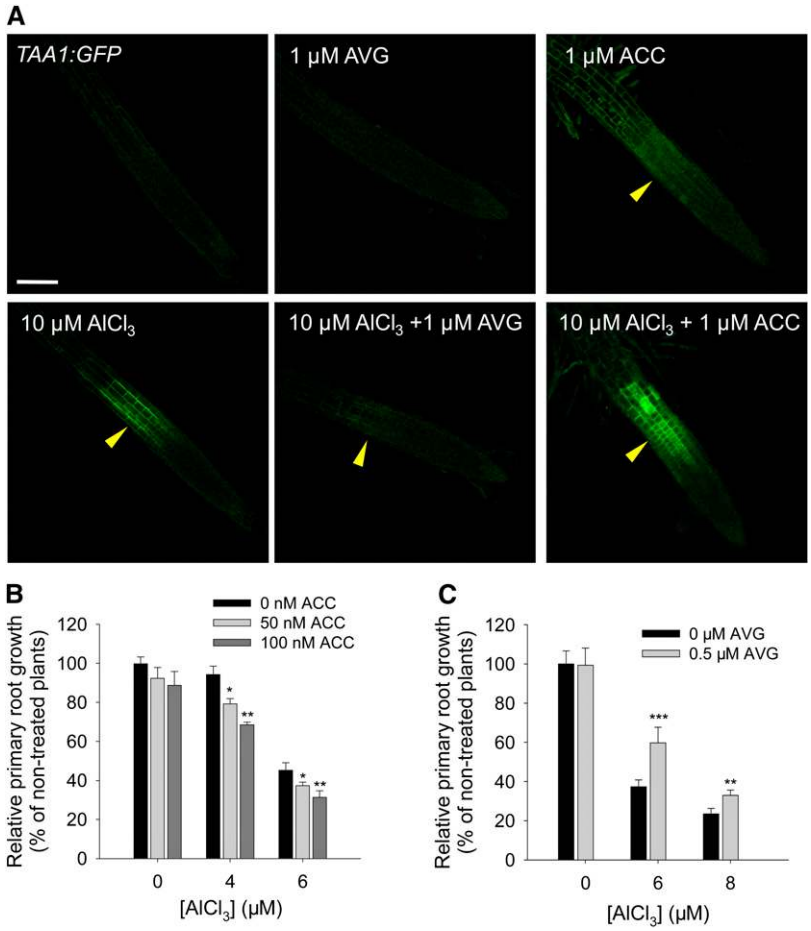

Figure 5. Al-Induced *TAA1* Expression in the TZ Is Regulated by Ethylene.

(A) Expression of the *TAA1:GFP* transgene in the epidermis of the root apex in the presence of Al plus ACC or AVG treatment. Four-day-old transgenic *TAA1:GFP* seedlings were pretreated without or with 1 μM AVG or 1 μM ACC for 2 d, and then the seedlings were continuously treated without or with 1 μM AVG or 1 μM ACC in the absence or presence of 10 μM $AlCl_3$ for 2 h. The TZ is marked by yellow arrowheads. Bar = 100 μm.
(B) and **(C)** Relative primary root growth of the wild type in the presence of 0, 4, and 6 μM $AlCl_3$ plus 0, 50, or 100 nM ACC **(B)** or 0, 6, and 8 μM $AlCl_3$ plus 0 or 0.5 μM AVG **(C)** for 7 d. Asterisks in **(B)** indicate that means within the ACC treatment differ significantly at *P < 0.05 and **P < 0.01 (*t* test). Asterisks in **(C)** indicate that means within the AVG treatment differ significantly at **P < 0.01 and ***P < 0.001 (*t* test). Values represent means ± SD (n = 30).

The *arf10/16* Double Mutant Has a Differential Transcriptional Program in Response to Al Treatment

To reveal how ARF10 and ARF16 regulate Al-induced root growth inhibition, a transcriptome analysis through RNAseq was performed by comparing the *arf10/16* double mutant line and the wild type in the presence and absence of Al (Supplemental Data Set 1), and a more detailed analysis of the transcriptome focused on the comparison of the Al-exposed *arf10/16* double mutant line and the wild type. In total, 207 genes were upregulated by at least 2-fold and 93 genes were downregulated by at least 2-fold in the root tissue of the double mutant compared with wild-type plants, both exposed to Al (Supplemental Figures 11A and 11B and Supplemental Data Sets 2 and 3). About 21% of the upregulated genes and 27% of the downregulated genes could not be functionally assigned. Among the upregulated genes, ~20% were involved in cell wall synthesis and organization, 12% in primary metabolic processes, 10% in each of transport and cellular protein metabolic/modification processes, 9% in each of transcription regulation and stress/defense, etc.; the downregulated genes were dominated by primary metabolic processes (15%), transport (13%), stress/defense (12%), transcription regulation (10%), cell wall synthesis and organization (7%), etc. The strong representation of cell wall synthesis and organization-related genes implied that the improved Al tolerance of the double mutant relied heavily on cell wall modifications. Among the 47 regulated cell wall–related genes, 22 encode structural cell wall proteins, specifically Hyp-rich glycoproteins (HRGPs), a group that includes the extensins, the arabinogalactan proteins, and the Pro-rich proteins (Supplemental Figure 11C and Supplemental Data Set 4). Thus, cell wall assembly appears to be important in the auxin-mediated response of the root to Al exposure. Differential transcription of genes in the categories glycosyl hydrolases (three upregulated and five downregulated), carbohydrate esterases (four upregulated), glycosyl transferases

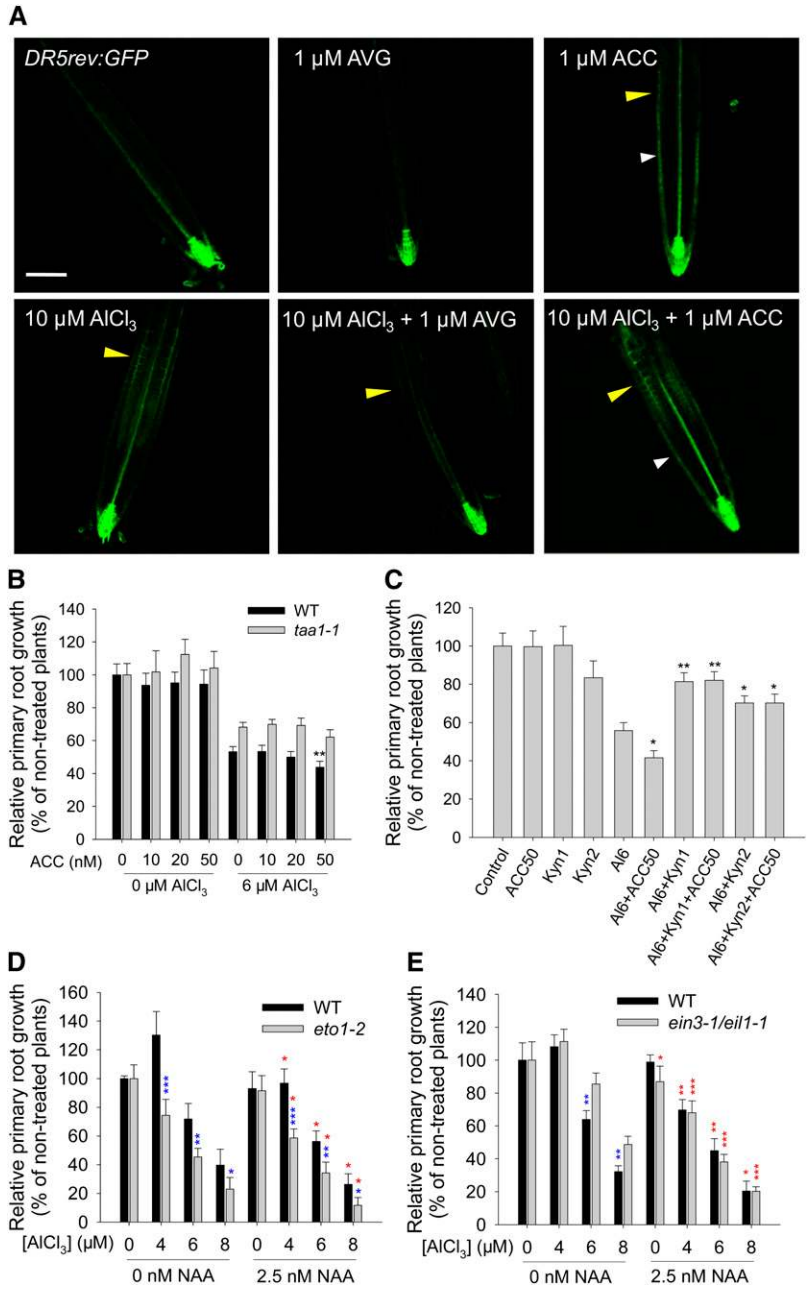

Figure 6. Ethylene Mediates TAA1-Regulated Local Auxin Response in the TZ in Response to Al Stress.

(A) Expression of the *DR5rev:GFP* transgene in the root apex in the presence of Al plus ACC or AVG treatment. Four-day-old transgenic *DR5rev:GFP* seedlings were pretreated without or with 1 μM AVG or 1 μM ACC for 2 d, and then the seedlings were continuously treated without or with 1 μM AVG or 1 μM ACC in the absence or presence of 10 μM $AlCl_3$ for 2 h. The TZ is marked by yellow arrowheads, and white arrowheads show DR5rev:GFP signals in the meristem zone. Bar = 100 μm.
(B) Relative primary root growth of the wild type and *taa1-1* in the presence of ACC (0, 10, 20, and 50 nM) and Al (0 and 6 μM $AlCl_3$) for 7 d. Asterisks indicate that means within the ACC treatment in the 6 μM $AlCl_3$–exposed *taa1-1* mutant differ at $^{**}P < 0.01$ (*t* test). Values represent means ± SD ($n = 30$).
(C) Relative primary root growth of the wild type in the presence of Al (0 and 6 μM $AlCl_3$) plus ACC (0 and 50 nM) and/or plus Kyn (0, 1, and 2 μM) for 7 d. Asterisks indicate that means within the ACC, Kyn, or Kyn plus ACC treatment in the 6 μM $AlCl_3$–exposed wild-type roots differ at $^{*}P < 0.05$ and $^{**}P < 0.01$ (*t* test). Values represent means ± SD ($n = 30$).
(D) and **(E)** Relative primary root growth of the wild type, *eto1-2*, and *ein3-1 eil1-1* in the presence of 0, 4, 6, and 8 μM $AlCl_3$ plus 0 and 2.5 nM NAA for 7 d. Blue asterisks indicate that wild-type and mutant means differ significantly at $^{*}P < 0.05$, $^{**}P < 0.01$, and $^{***}P < 0.001$; red asterisks indicate that wild-type and mutant means within the NAA treatment in each Al concentration differ significantly at $^{*}P < 0.05$, $^{**}P < 0.01$, and $^{***}P < 0.001$ (*t* test). Values represent means ± SD ($n = 30$).

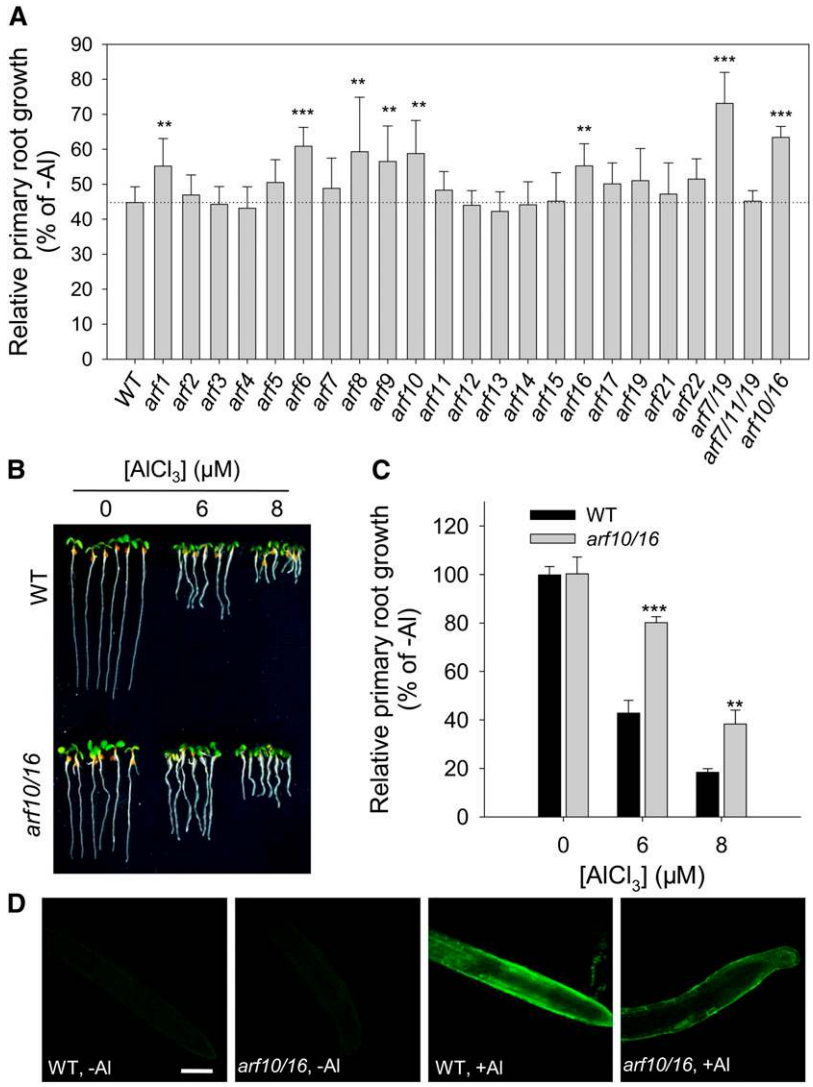

Figure 7. ARFs Mediate the Al-Induced Inhibition of Root Growth.

(A) Relative primary root growth of *arf* mutants exposed for 7 d to either 0 or 6 μM $AlCl_3$. Asterisks indicate that wild-type and mutant means differ significantly at **P < 0.01 and ***P < 0.001 (*t* test). Values represent means ± SD (n = 30).

(B) and **(C)** Root growth of wild-type and *arf10/16* double mutant plants following a 7-d exposure to 0, 6, or 8 μM $AlCl_3$. Asterisks in **(C)** indicate that wild-type and double mutant means differ significantly at **P < 0.01 and ***P < 0.001 (*t* test). Values in **(C)** represent means ± SD (n = 30).

(D) Morin staining illustrates the accumulation of Al in the root tip of 6-d-old wild-type and *arf10/16* double mutant seedlings exposed to 10 μM $AlCl_3$ for 24 h. Bar = 100 μm.

[See online article for color version of this figure.]

(two upregulated), and polysaccharide lyases (two upregulated) (Supplemental Figure 11C and Supplemental Data Set 4) also suggests the importance of cell wall modification.

For validation, the transcription of a set of 40 of the differentially transcribed genes putatively involved in the determination of cell wall properties was characterized using qRT-PCR. The correlation between the RNAseq and qRT-PCR data was highly significant (r^2 = 0.85, P < 0.001) (Supplemental Figure 11D). The rapid binding of Al to the cell wall matrix is expected to alter the properties of the cell wall and thereby affect root growth (Tabuchi and Matsumoto, 2001; Ma et al., 2004; Horst et al., 2010; Yang et al., 2013). Several genes related to cell wall structure and composition, including those encoding xyloglucanases, endotransglycosylases, polygalacturonases, and glycosyl transferases, have been identified as being involved in the regulation of Al tolerance or the Al-induced inhibition of root growth (Kumari et al., 2008; Maron et al., 2008; Tsutsui et al., 2012; Zhu et al., 2012). Among the 40 genes whose transcription was monitored using qRT-PCR in both wild-type and double mutant plants, either exposed or not exposed to Al for 24 h, 26 genes (17 encoding HRGPs, 4 encoding

carbohydrate esterases, 3 encoding glycosyl hydrolases, and 1 each encoding polysaccharide lyase and glycosyl transferase) with relatively high expressional changes were identified. Nearly all of these genes were strongly downregulated by Al, especially in the wild-type plants but less so in the double mutant. The exceptions were genes encoding glycosyl hydrolases, which were either not affected by the Al treatment or were upregulated (but less so in the double mutant than in the wild type) (Figures 8A and 8B).

It has been established that *ALUMINUM-ACTIVATED MALATE TRANSPORTER1* (*ALMT1*), a gene that encodes a malate transporter, and *MULTIDRUG AND TOXIN EXTRUSION FAMILY PROTEIN* (*MATE*), which encodes a citrate transporter, are required for the exudation from the root of malate and citrate, respectively, a process associated with improved Al resistance (Liu et al., 2009). The RNAseq analysis revealed that the loss of both *ARF10* and *ARF16* function had no effect on the transcript

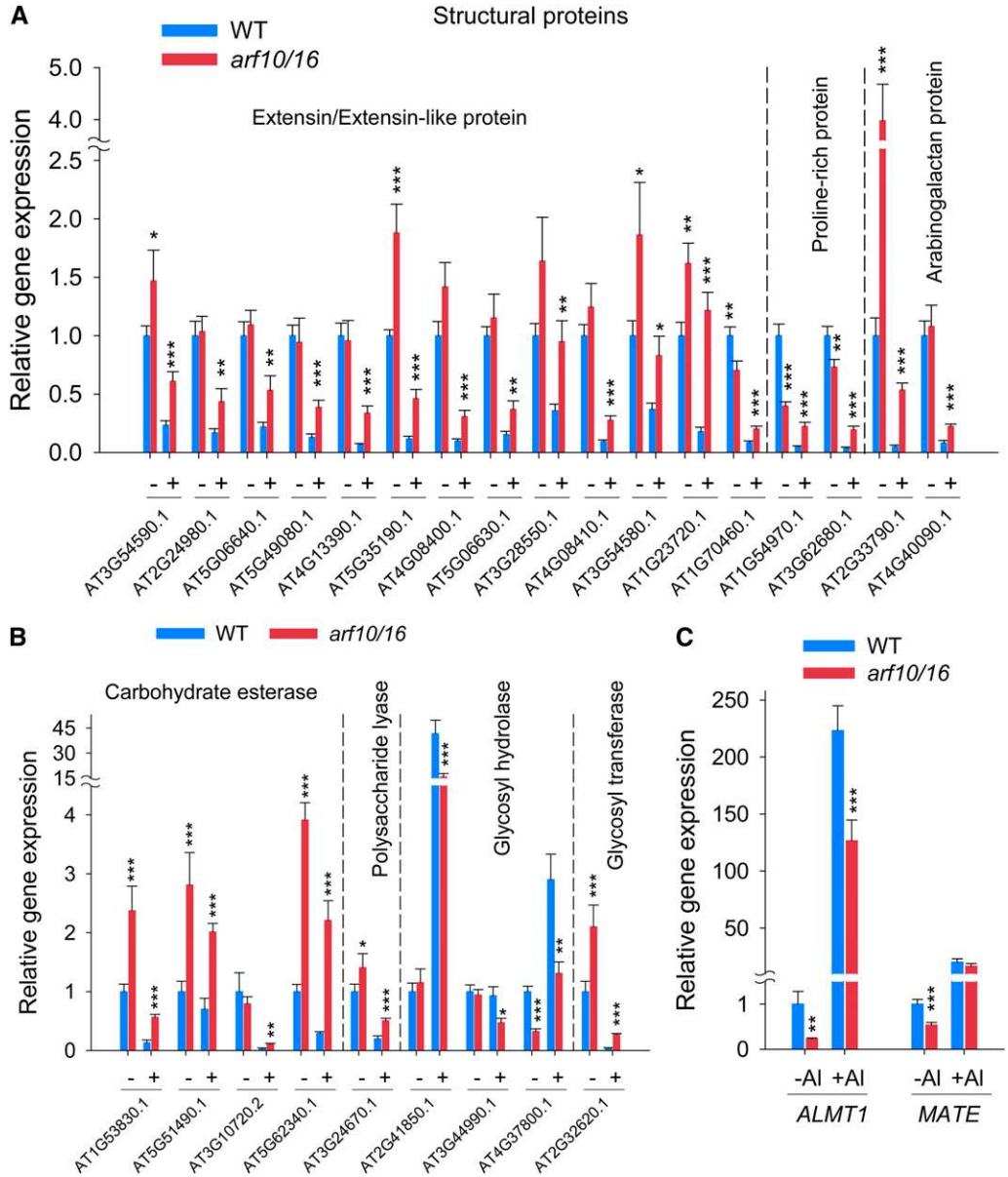

Figure 8. Transcriptional Analysis Based on qRT-PCR.

(A) and **(B)** Gene expression of cell wall–related genes predicted to be involved in the *ARF10/16*-mediated Al-induced inhibition of root growth.
(C) Expression of the Al resistance–associated genes *ALMT1* and *MATE*.
Six-day-old seedlings were exposed to 10 μM $AlCl_3$ for 24 h. *UBQ1* was used as the reference, and a nontreated wild type was used as the sample control. Values represent means ± SE ($n = 3$). Asterisks indicate that wild-type and *arf10/16* mutant means differ significantly at *P < 0.05, **P < 0.01, and ***P < 0.001 (*t* test).
[See online article for color version of this figure.]

abundance of *MATE* and even suppressed that of *ALMT1* (Supplemental Data Sets 2 and 3). The qRT-PCR analysis showed that the Al treatment strongly upregulated *ALMT1* in both the double mutant and the wild type and that the abundance of *ALMT1* transcript was substantially lower in the double mutant than in the wild type, regardless of whether the plants were exposed to Al (Figure 8C). The transcription of *MATE* was also enhanced by exposure to Al, but it remained at a lower level in the double mutant than in the wild type in the absence of Al. Therefore, it is considered unlikely that the reduced Al-induced root growth inhibition of the double mutant compared with the wild type can be explained by a greater malate or citrate exudation.

DISCUSSION

Auxin is a prime regulator of root cell division, elongation, and differentiation and, hence, overall root growth. High concentrations of auxin, however, inhibit the elongation of certain cell types (Teale et al., 2005). Auxin signaling within the root-apex TZ is sensitive not only to developmental signals but also to environmental cues (Baluška et al., 2010), including Al (Sivaguru and Horst, 1998). Until now, how external Al interacts with the root-apex TZ to inhibit root growth has been unclear. The importance of the basipetal transport of auxin from the meristematic zone through the TZ and into the EZ in driving the Al-induced inhibition of root elongation in maize has been highlighted by Kollmeier et al. (2000). Since the external supply of auxin to the EZ is able to partially overcome the inhibition of root growth imposed by the application of Al to the TZ, the suggestion was made that the EZ suffers from auxin deficiency.

In *Arabidopsis*, TAA1-mediated localized auxin biosynthesis has been reported to be involved in shade avoidance and root growth and development (Stepanova et al., 2008; Tao et al., 2008). Here, a combination of appropriate mutants and the use of a specific signaling transgene have demonstrated that both manipulating the internal auxin level and interfering with the auxin signaling pathway affect the Al-induced inhibition of root growth via auxin signaling in the root-apex TZ, and this process largely depends on TAA1-regulated localized auxin biosynthesis. Auxin alleviates the Al-induced inhibition of the elongation of the maize EZ (Kollmeier et al., 2000), while, by contrast, it enhances the Al-induced inhibition of root growth in *Arabidopsis*. Such a fundamental difference may well reflect a diversity of target sites for Al, since in monocotyledonous species such as maize and sorghum, Al sensitivity is restricted to the TZ (Sivaguru and Horst, 1998; Sivaguru et al., 1999, 2013), while in the dicotyledonous species common bean, both the TZ and the EZ are sensitive (Rangel et al., 2007). The observation that toxic levels of Al drive up the endogenous level of auxin in the common bean root tip (including the meristematic zone, TZ, and EZ) (Yang et al., 2012), in agreement with our findings here in *Arabidopsis* root tips (Figure 1B), provides some corroboration for Al-induced enhanced auxin signaling in the *Arabidopsis* root-apex TZ.

For the moment, it cannot be excluded that polar transport of auxin could also contribute to the Al-induced accumulation of auxin in the root TZ, since root growth in *pin1-5* is significantly more inhibited by Al than in the wild type (Supplemental Figure 12). How polar transport of auxin mediates Al-induced root growth inhibition needs to be substantiated by further, more detailed studies. However, this investigation shows that TAA1-mediated local auxin synthesis in the TZ is crucial for the Al-induced inhibition of root growth. The auxin accumulation in the TZ mimics the root growth inhibition induced by an external supply of auxin, much of which is taken up by the TZ (Schlicht et al., 2006). A recent report, which showed that auxin enhances Al toxicity via an alteration in *ALUMINUM-SENSITIVE1*–mediated Al distribution (Zhu et al., 2013), provides further support for our findings. Unfortunately, the study of Zhu et al. (2013) made no attempt to define the spatial correlations between Al and auxin effects in the root apex during the Al-induced inhibition of root growth.

The role of the auxin–ethylene interaction in regulating the growth and development of seedlings has been proposed earlier (Pickett et al., 1990), well investigated (Růzicka et al., 2007; Stepanova et al., 2007, 2011; Swarup et al., 2007), and reviewed recently by Muday et al. (2012). Similar to auxin, which has long been known to play a critical role in Al-induced root growth inhibition (Kollmeier et al., 2000; Sun et al., 2010), ethylene has also been reported to be important in Al-induced root growth inhibition in common bean (Massot et al., 2002; Eticha et al., 2010), *Lotus japonicus* (Sun et al., 2007), *Arabidopsis* (Sun et al., 2010), and wheat (*Triticum aestivum*; Tian et al., 2014b). Also, the potential participation of the auxin–ethylene interaction in the regulation of Al-induced root growth

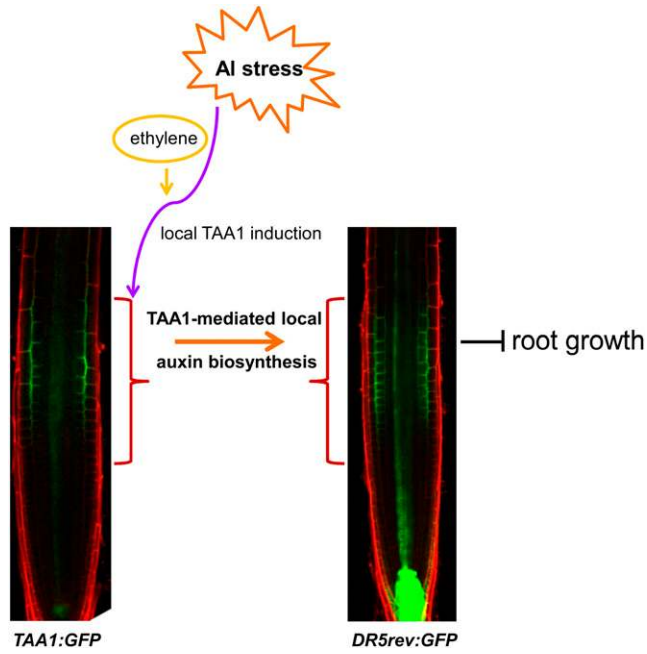

Figure 9. Schematic Representation of TAA1-Regulated Local Auxin Biosynthesis in the TZ Mediating Root Growth Inhibition in Response to Al Stress.

Al stress induces *TAA1* local upregulation (shown by *TAA1:GFP*) in the TZ through an ethylene-dependent pathway, thus inducing local auxin accumulation and an auxin signaling maximum in the TZ (shown by *DR5rev:GFP*) and inhibition of root growth.

inhibition has been suggested (Sun et al., 2010; Tian et al., 2014b), while the exact interaction mechanism during Al-induced inhibition of root growth is still undetermined. Here, our results indicate that, in response to Al stress, ethylene induces local *TAA1* upregulation and thus the auxin signaling maximum in the root-apex TZ, inducing root growth inhibition (Figure 9).

ARFs bind to auxin response elements in promoters of early auxin response genes and are crucial for mediating auxin signaling (Guilfoyle and Hagen, 2007). Loss-of-function *ARF* mutants revealed that *arf1*, *arf6*, *arf8*, *arf9*, *arf10*, and *arf16*, and particularly the double mutants *arf7/19* and *arf10/16*, showed greater Al resistance than the wild type (Figure 7A). The analysis of tissue expression pattern demonstrated that *ARF10* and *ARF16*, which were regulated by the Al-modulated miR160 (Wang et al., 2005; Liu et al., 2007; Liu et al., 2010; Chen et al., 2012; Zeng et al., 2012), were highly expressed in the epidermis and cortex of the root apex (Supplemental Figure 10; Rademacher et al., 2011; Baster et al., 2013), the major Al perception site (Ryan et al., 1993), suggesting the potential involvement of ARF10 and ARF16 in auxin-mediated Al-induced inhibition of root growth. However, no transcriptional change was found for *ARF10* and *ARF16* under Al stress on the entire root basis (Supplemental Data Set 1).

The transcriptomic analysis presented here revealed that many of the differentially transcribed genes associated with cell wall modification were regulated by the transcription factors ARF10 and ARF16. The implication is that the auxin-regulated Al-induced inhibition of root growth arises from auxin signaling–regulated modification of cell wall structure or components. The importance of the properties of the cell wall in the context of Al-induced inhibition of root elongation and in Al tolerance has been emphasized (Horst et al., 2010). The binding of Al to the cell wall, and particularly to the pectic and hemicellulosic matrix in the most Al-sensitive zone of the root apex, has a major effect on cell wall properties and root growth in *Arabidopsis* (Yang et al., 2011a; Yang et al., 2011b; Zhu et al., 2012, 2013). The binding of Al to pectins is known to be highly dependent on their degree of methylation: binding occurs preferentially to unmethylated pectin, catalyzed by the activity of pectin methylesterase (PME) (Horst et al., 2010; Yang et al., 2011b). These enzymes are regulated by specific inhibitors (PMEIs). Group 2 PMEs contain, in addition to the catalytic domain, an N-terminal extension domain, PRO, which has some similarity to known PMEI domains such as *PME2* (Gribaa et al., 2013). The clearly higher transcript abundance of two *PMEI* family genes and two genes coding for PMEI domain–containing proteins in the roots of the *arf10/16* double mutant exposed to Al (Figure 8; Supplemental Data Set 4) may reflect a higher degree of pectin methylation and, thus, a reduced rate of Al accumulation (Figure 7D) compared with wild-type roots.

The upregulation of cell wall–related genes in the *arf10/16* double mutant primarily encoding cell wall structure proteins, including HRGPs, arabinogalactan proteins, and various Pro- and Gly-rich proteins, suggests that its reduced sensitivity to Al-induced inhibition of root growth is probably the outcome of a complex network including structure assembly and remodeling. A potential role for HRGPs in Al tolerance in rice (*Oryza sativa*) has been suggested by Pan et al. (2011), although no mechanistic basis has yet been proposed. One possibility is that the Al-induced accumulation of HRGPs may alter cell wall porosity and, as a result, reduce the mobility of Al in the root apoplast (Yang et al., 2011b). The plant cell wall is a developmentally dynamic structure that also responds to various external stimuli (Farrokhi et al., 2006). Thus, once the cell wall structure proteins have been deposited, the expression of genes involved in wall polysaccharide remodeling (such as those encoding glycosyl hydrolases and polysaccharide lyases) can be expected to be promoted, as was indeed the case (Figure 8B; Supplemental Data Set 4). An outcome of this burst of gene expression is to facilitate cell wall enlargement (Gribaa et al., 2013). The upregulation of *CELLULOSE SYNTHASE-LIKE PROTEIN B2*, coding for a protein involved in cellulose synthesis, may have led to the reduced inhibition of growth in the double mutant roots, while the repression of *XTH31* and *XTH7*, genes that encode xyloglucan endotransglucosylase/hydrolases, may have alleviated Al toxicity by reducing the xyloglucan content of the cell wall, thereby lowering its Al binding capacity (Zhu et al., 2012).

The malate transporter ALMT1 and the citrate transporter MATE are known to improve Al resistance by promoting the exudation of malate/citrate from the *Arabidopsis* root (Liu et al., 2009). The change in transcript abundance of *ALMT1* and *MATE* in the roots of the *arf10/16* double mutant in response to Al exposure (Figure 8C) does not support the assumption that the reduced Al-induced inhibition of root growth resulted from an enhanced malate and/or citrate exudation. Kobayashi et al. (2013) described how externally supplied IAA enhances both *ALMT1* and *MATE* transcription, which, however, did not affect malate exudation, while in the IAA signaling double mutant line *nonphototropic hypocotyls4-1 auxin-responsive factor19-1* (synonymous with *arf7/19*), the Al-induced expression of *ALMT1* remained unaltered. Thus, it appears that the mechanism for auxin signaling–regulated Al toxicity might be independent of organic acid anion exudation.

In conclusion, this study provides evidence that the TAA1-mediated local auxin biosynthesis is responsible for the Al-induced inhibition of root growth. The mechanistic basis for the process operates via the mediation of the auxin response depending on ethylene-regulated TAA1 expression in the root-apex TZ and, thus, downstream signaling regulation via ARF transcription factors. Cell wall modification is probably a further downstream response to Al exposure and contributes to the auxin-mediated root growth inhibition in response to Al stress. The wider picture illustrates how hormone signaling can regulate root growth plasticity in response to environmental cues, providing a general mechanism for plants to adapt to a changing environment.

METHODS

Plant Material and Growth Conditions

Arabidopsis thaliana ecotype Columbia, mutant lines *yuc1D* (Zhao et al., 2001), *slr-1* (Fukaki et al., 2005; Vanneste et al., 2005), *PIN8 OX* (Ding et al., 2012), *taa1-1* (CS66987), *eto1-2* (He et al., 2011), *ein3-1 eil1-1* (Alonso et al., 2003; He et al., 2011), *arf1* to *arf22* (except *arf18* and *arf20*) (Mai et al., 2011), *arf7/19* (Okushima et al., 2007), *arf10/16* (Ding and Friml, 2010), *arf7/11/19*, *DR5rev:GFP* (Ding and Friml, 2010), *TAA1:GFP-TAA1* (Stepanova et al., 2008), and *DR5rev:GFP/taa1-1* were used in this study. Seedlings were grown hydroponically as described by Kobayashi et al. (2007) in 2% strength modified MGRL (Fujiwara et al., 1992) solution (but with Pi eliminated and the Ca concentration adjusted to 200 μM) at pH 5.0 in a growth chamber with a 16/8-h light/dark cycle at 22°C.

Treatments and Root Growth Analysis

In this study, pH 5.0 medium was selected to prevent the precipitation of Al in the medium as described by Iuchi et al. (2007) and also because of the hypersensitivity of *Arabidopsis* root growth to low pH (Supplemental Figure 7). Although we attempted to maintain the pH constant by frequent adjustment, we cannot exclude the possibility that the pH occasionally decreased slightly below the target pH, which may explain why Al-induced root growth inhibition varied between experiments. For root growth experiments, the seeds were sown onto polypropylene mesh floating on 2% modified MGRL solution containing Al (total [$AlCl_3$] 0 to 8 μM, pH 5.0) or Al plus PEO-IAA (gifts from Ken-ichiro Hayashi), NAA, Kyn, ACC, or AVG (pH 5.0) or various pH treatments (pH 4.2 to 5.5) for 7 d. The solution was renewed every 2 d. At day 7, the roots were scanned and primary root length was calculated with ImageJ software.

For short-term treatments, the seedlings were pregrown in 2% modified MGRL solution for 6 d and then transferred to different Al treatment solutions ([$AlCl_3$] 10 or 25 μM, pH 5.0) or various pH stress solutions (pH 4.2 to 5.5) for 2 h. The free Al^{3+} activity in 2% MGRL solution with [$AlCl_3$] 1, 2, 3, 4, 5, 6, 8, 10, and 25 μM at pH 5.0 is 0.0006, 0.27, 0.66, 1.1, 1.4, 1.8, 2.6, 3.4, and 9.4 μM, respectively, calculated using GEOCHEM-EZ software (http://www.plantmineralnutrition.net/Geochem/geochem%20home.htm).

Confocal Microscopy

Imaging was performed on an LSM-700 laser-scanning confocal microscope (Zeiss). For visualization of the expression of *DR5rev:GFP* and *TAA1:GFP* in roots, 6-d-old plants were treated with $AlCl_3$ ([$AlCl_3$] 0 and 10 μM) or various pH values for 2 h, and then roots were mounted with PI. For visualization of Al in the root tips, after $AlCl_3$ treatment ([$AlCl_3$] 0 and 10 μM) for 24 h, the excised roots were washed in MES buffer (pH 5.5) for 10 min, stained with 100 μM morin in the same buffer for 1 h with gentle shaking, and washed several times with MES buffer, and the green Al-morin fluorescence signal was then observed. Cell viability was determined by PI/FDA staining; living cells generate green fluorescence when stained in FDA, while nuclei of membrane-compromised cells will show red PI fluorescence as a sign of cell death.

IAA Concentration Determination

Six-day-old wild-type seedlings were treated with 6 μM $AlCl_3$ at pH 5.0 for 0, 3, 6, and 12 h. Then, 1-mm-long root tips were excised and immediately frozen in liquid nitrogen. Root tips were ground to powder in liquid nitrogen. Afterward, 1 mL of 80% (v/v) methanol was added to each sample and vortexed. The IAA in root tips was extracted, and the concentration was determined according to Zhou et al. (2010) by gas chromatography–mass spectrometry.

RNA Isolation and qRT-PCR

Approximately 500 seedlings were grown in 2% modified MGRL nutrient solution for 6 d, and then the plants were treated with $AlCl_3$ ([$AlCl_3$] 0 and 10 μM) for 24 h. The roots were rinsed with distilled water, harvested, and shock-frozen in liquid nitrogen. Total RNA was isolated using TriPure isolation reagent (Roche), and first-strand cDNA was synthesized from 1 μg of total RNA using the Transcriptor First Strand cDNA Synthesis Kit (Roche) following the manufacturer's protocol. qRT-PCR was performed using the CFX Connect Real-Time System (Bio-Rad) with FastStart Universal SYBR Green Master (Rox) (Roche). Samples for qRT-PCR were run in three biological replicates and two technical replicates. For the normalization of gene expression, the ubiquitin gene *UBQ1* (*AT3G52590*) was used as an internal standard, and the nontreated wild type was used as a sample control. Primers were designed using Primer 5 software, and the specifications of the primers of the genes studied are given in Supplemental Data Set 5.

RNAseq Analysis

The RNAseq analysis was performed by BGI Tech. Approximately 500 seedlings (6 d old) of both the wild-type Columbia and the *arf10/16* double mutant line were exposed to a 2% MGRL solution containing 0 or 10 μM $AlCl_3$ (pH 5.0). After 24 h, the roots were sampled for RNA isolation. Total RNA was isolated using the RNeasy Plant Mini Kit (Qiagen) following the manufacturer's protocol. The isolated total RNA samples were treated with DNase I to degrade any possible DNA contamination and enriched using oligo(dT) magnetic beads (for eukaryotes) or by removing rRNAs from the total RNA (for prokaryotes). Mixed with the fragmentation buffer, the mRNA was fragmented into short fragments (~200 bp). Then, the first strand of cDNA was synthesized by using random hexamer primer. Buffer, deoxynucleotide triphosphates, RNase H, and DNA polymerase I were added to synthesize the second strand. The double-stranded cDNA was purified with magnetic beads. End reparation and 3′ end single nucleotide A (adenine) addition were then performed. Finally, sequencing adaptors were ligated to the fragments. The fragments were enriched by PCR amplification. The constructed sample libraries were qualified and quantified with an Agilent 2100 Bioanaylzer and the ABI StepOnePlus Real-Time PCR System and then sequenced via Illumina HiSeq 2000 or other sequencer when necessary.

The raw reads were obtained by transferring the original image data produced by the sequencer into sequences by base calling. The raw reads were then cleaned by removing the low-quality reads and/or adaptor sequences. The clean reads with high-quality sequences were mapped to reference sequences and/or the reference gene set using SOAPaligner/SOAP2 (Li et al., 2009). No more than two mismatches were allowed in the alignment.

The gene expression levels were calculated using the reads per kilobase per million reads method (Mortazavi et al., 2008). Differentially expressed genes (DEGs) within samples were screened with a modified method according to Audic and Claverie (1997). Statistical analysis of DEGs was conducted using the P value and the false discovery rate (FDR). The P value corresponds to the differential gene expression test. FDR is a method used to determine the threshold of P values in multiple tests (Benjamini and Yekutieli, 2001). FDR $\leq$ 0.001 and absolute value of $\log_2$ ratio $\geq$ 1 were used as the threshold to judge the significance of gene expression differences. The functional categories of the DEGs were BLASTed against the nonredundant GenBank, KEGG Pathway, and UniProt protein databases by the Gene Ontology annotation.

Statistical Analysis

Statistical analysis was performed using SAS 9.2 (SAS Institute). Means were compared using Student's *t* test. Asterisks in the figures denote significant differences as follows: *P < 0.05, **P < 0.01, and ***P < 0.001.

Accession Numbers

Sequence data from this article can be found in the Arabidopsis Genome Initiative database and the GenBank/EMBL databases under the following accession numbers: *SLR* (AT4G14550, AF334718), *YUC1* (AT4G32540, NM_119406), *PIN8* (AT5G15100, NM_121514), *TAA1* (AT1G70560, NM_105724), *ETO1* (AT3G51770, NM_001035762), *EIN3* (AT3G20770, NM_112968), *EIL1* (AT2G27050, BT003344), *ARF10* (AT2G28350, AF325073), *ARF16* (AT4G30080, AY059792), *ALMT1* (AT1G08430, NM_100716), and *MATE* (At1g51340, AY059793). RNA sequencing data analyzed in this study are available in the Gene Expression Omnibus database under accession number GSE57487.

Supplemental Data

The following materials are available in the online version of this article.

Supplemental Figure 1. The Root-Apex TZ Is the Major Site of Al Sensitivity, as Indicated by PI and FDA Staining.

Supplemental Figure 2. Time-Course Response of the Expression of *DR5rev:GFP* in Root Apex Exposed to Al Stress.

Supplemental Figure 3. Short-Term Effect of PEO-IAA on Al-Induced Inhibition of Root Growth.

Supplemental Figure 4. Effect of Exogenous NAA on Al-Induced *DR5rev:GFP* Expression in Root Apex.

Supplemental Figure 5. Effect of Exogenous NAA on the Expression of Auxin-Responsive Genes in Al-Exposed Roots.

Supplemental Figure 6. Temporal Analysis of Al-Induced Expression of *TAA1:GFP* in Root Apex.

Supplemental Figure 7. The Sensitivity of the *Arabidopsis* Root to Low pH.

Supplemental Figure 8. The pH of the Medium Has No Effect on the Expression of Either the *DR5rev:GFP* or the *TAA1:GFP* Transgene.

Supplemental Figure 9. Effect of ACC and AVG on the Expression of *DR5rev:GFP* Transgene in the Root Apex under Al Stress.

Supplemental Figure 10. The Expression Pattern of *ARFs:GFP* Transgene in the Root Apex.

Supplemental Figure 11. Transcriptomic Analysis of the Response to Al Exposure.

Supplemental Figure 12. Phenotype Analysis of Root Growth of Polar Auxin Transport–Related Mutants in Response to Al Stress.

Supplemental Data Set 1. Comparison of the Differentially Expressed Genes in Roots of the Wild Type and *arf10/16* Exposed to Al Stress though RNAseq Analysis.

Supplemental Data Set 2. Upregulated Genes in Roots of *arf10/16* Double Mutants.

Supplemental Data Set 3. Downregulated Genes in Roots of *arf10/16* Double Mutants.

Supplemental Data Set 4. List of Differential Expressed Genes (DEGs) Involved in Cell Wall Synthesis and Organization in Roots of *arf10/16* Double Mutants.

Supplemental Data Set 5. List of Genes and Specific Primer Pairs Used for Quantitative Real-Time PCR (qRT-PCR).

ACKNOWLEDGMENTS

We thank Ken-ichiro Hayashi for PEO-IAA chemicals. We thank Jiri Friml, Jose Alonso, Tom Beeckman, Hongwei Guo, Dolf Weijers, Guang-qin Guo, and Hong-quan Yang for published materials. We also thank the editor and anonymous reviewers for their constructive comments and insightful suggestions, which greatly improved this article. Z.D. is supported by the National Natural Science Foundation of China (Grants 31270327 and 31222005), the 1000-Talents Plan from China for young researchers (Grant 104.206.99.99), and Qilu Scholarship from Shandong University of China (Grant 11200081963024). Z.-B.Y. is supported by the Independent Innovation Fund project of Shandong University (Grant 2012HW005) and the China Postdoctoral Science Foundation (Grants 2012M521322 and 2013T60664).

AUTHOR CONTRIBUTIONS

Z.D. and Z.-B.Y. conceived the study and designed the experiments. Z.-B.Y., Z.D., X.G., C.H., and R.W. performed the experiments and analyzed the data. Z.D., Z.-B.Y., and W.J.H. wrote the article. All authors discussed the results and commented on the article.

Received May 21, 2014; revised June 18, 2014; accepted June 28, 2014; published July 22, 2014.

REFERENCES

Alonso, J.M., Stepanova, A.N., Solano, R., Wisman, E., Ferrari, S., Ausubel, F.M., and Ecker, J.R. (2003). Five components of the ethylene-response pathway identified in a screen for weak ethylene-insensitive mutants in Arabidopsis. Proc. Natl. Acad. Sci. USA **100:** 2992–2997.

Audic, S., and Claverie, J.M. (1997). The significance of digital gene expression profiles. Genome Res. **7:** 986–995.

Baluška, F., Mancuso, S., Volkmann, D., and Barlow, P.W. (2010). Root apex transition zone: A signalling-response nexus in the root. Trends Plant Sci. **15:** 402–408.

Baster, P., Robert, S., Kleine-Vehn, J., Vanneste, S., Kania, U., Grunewald, W., De Rybel, B., Beeckman, T., and Friml, J. (2013). SCF(TIR1/AFB)-auxin signalling regulates PIN vacuolar trafficking and auxin fluxes during root gravitropism. EMBO J. **32:** 260–274.

Benjamini, Y., and Yekutieli, D. (2001). The control of the false discovery rate in multiple testing under dependency. Ann. Stat. **29:** 1165–1188.

Benková, E., and Hejátko, J. (2009). Hormone interactions at the root apical meristem. Plant Mol. Biol. **69:** 383–396.

Bielach, A., Duclercq, J., Marhavý, P., and Benková, E. (2012). Genetic approach towards the identification of auxin-cytokinin crosstalk components involved in root development. Philos. Trans. R. Soc. Lond. B Biol. Sci. **367:** 1469–1478.

Chen, L., Wang, T., Zhao, M., Tian, Q., and Zhang, W.H. (2012). Identification of aluminum-responsive microRNAs in *Medicago truncatula* by genome-wide high-throughput sequencing. Planta **235:** 375–386.

Delhaize, E., and Ryan, P.R. (1995). Aluminum toxicity and tolerance in plants. Plant Physiol. **107:** 315–321.

Ding, Z., and De Smet, I. (2013). Localised ABA signalling mediates root growth plasticity. Trends Plant Sci. **18:** 533–535.

Ding, Z., and Friml, J. (2010). Auxin regulates distal stem cell differentiation in *Arabidopsis* roots. Proc. Natl. Acad. Sci. USA **107:** 12046–12051.

Ding, Z., et al. (2012). ER-localized auxin transporter PIN8 regulates auxin homeostasis and male gametophyte development in *Arabidopsis*. Nat. Commun. **3:** 941–949.

Doncheva, S., Amenós, M., Poschenrieder, C., and Barceló, J. (2005). Root cell patterning: A primary target for aluminium toxicity in maize. J. Exp. Bot. **56:** 1213–1220.

Duan, L., Dietrich, D., Ng, C.H., Chan, P.M., Bhalerao, R., Bennett, M.J., and Dinneny, J.R. (2013). Endodermal ABA signaling promotes lateral root quiescence during salt stress in *Arabidopsis* seedlings. Plant Cell **25:** 324–341.

Eticha, D., Zahn, M., Bremer, M., Yang, Z., Rangel, A.F., Rao, I.M., and Horst, W.J. (2010). Transcriptomic analysis reveals differential gene expression in response to aluminium in common bean (*Phaseolus vulgaris*) genotypes. Ann. Bot. (Lond.) **105:** 1119–1128.

Farrokhi, N., Burton, R.A., Brownfield, L., Hrmova, M., Wilson, S.M., Bacic, A., and Fincher, G.B. (2006). Plant cell wall biosynthesis: Genetic, biochemical and functional genomics approaches to the identification of key genes. Plant Biotechnol. J. **4:** 145–167.

Fujiwara, T., Hirai, M.Y., Chino, M., Komeda, Y., and Naito, S. (1992). Effects of sulfur nutrition on expression of the soybean seed storage protein genes in transgenic petunia. Plant Physiol. **99:** 263–268.

Fukaki, H., Nakao, Y., Okushima, Y., Theologis, A., and Tasaka, M. (2005). Tissue-specific expression of stabilized SOLITARY-ROOT/IAA14 alters lateral root development in Arabidopsis. Plant J. **44:** 382–395.

Fukaki, H., Tameda, S., Masuda, H., and Tasaka, M. (2002). Lateral root formation is blocked by a gain-of-function mutation in the *SOLITARY-ROOT/IAA14* gene of *Arabidopsis*. Plant J. **29:** 153–168.

Gifford, M.L., Dean, A., Gutierrez, R.A., Coruzzi, G.M., and Birnbaum, K.D. (2008). Cell-specific nitrogen responses mediate developmental plasticity. Proc. Natl. Acad. Sci. USA **105:** 803–808.

Gribaa, A., Dardelle, F., Lehner, A., Rihouey, C., Burel, C., Ferchichi, A., Driouich, A., and Mollet, J.C. (2013). Effect of water deficit on the cell wall of the date palm (*Phoenix dactylifera* 'Deglet nour', Arecales) fruit during development. Plant Cell Environ. **36:** 1056–1070.

Guilfoyle, T.J., and Hagen, G. (2007). Auxin response factors. Curr. Opin. Plant Biol. **10:** 453–460.

Hayashi, K. (2012). The interaction and integration of auxin signaling components. Plant Cell Physiol. **53:** 965–975.

Hayashi, K., Tan, X., Zheng, N., Hatate, T., Kimura, Y., Kepinski, S., and Nozaki, H. (2008). Small-molecule agonists and antagonists of F-box protein-substrate interactions in auxin perception and signaling. Proc. Natl. Acad. Sci. USA **105:** 5632–5637.

He, W., et al. (2011). A small-molecule screen identifies L-kynurenine as a competitive inhibitor of TAA1/TAR activity in ethylene-directed auxin biosynthesis and root growth in *Arabidopsis*. Plant Cell **23:** 3944–3960.

Horst, W.J., Wang, Y., and Eticha, D. (2010). The role of the root apoplast in aluminium-induced inhibition of root elongation and in aluminium resistance of plants: A review. Ann. Bot. (Lond.) **106:** 185–197.

Illés, P., Schlicht, M., Pavlovkin, J., Lichtscheidl, I., Baluška, F., and Ovečka, M. (2006). Aluminium toxicity in plants: Internalization of aluminium into cells of the transition zone in *Arabidopsis* root apices related to changes in plasma membrane potential, endosomal behaviour, and nitric oxide production. J. Exp. Bot. **57:** 4201–4213.

Iuchi, S., Koyama, H., Iuchi, A., Kobayashi, Y., Kitabayashi, S., Kobayashi, Y., Ikka, T., Hirayama, T., Shinozaki, K., and Kobayashi, M. (2007). Zinc finger protein STOP1 is critical for proton tolerance in *Arabidopsis* and coregulates a key gene in aluminum tolerance. Proc. Natl. Acad. Sci. USA **104:** 9900–9905.

Jansen, L., Roberts, I., De Rycke, R., and Beeckman, T. (2012). Phloem-associated auxin response maxima determine radial positioning of lateral roots in maize. Philos. Trans. R. Soc. Lond. B Biol. Sci. **367:** 1525–1533.

Kobayashi, Y., Hoekenga, O.A., Itoh, H., Nakashima, M., Saito, S., Shaff, J.E., Maron, L.G., Piñeros, M.A., Kochian, L.V., and Koyama, H. (2007). Characterization of *AtALMT1* expression in aluminum-inducible malate release and its role for rhizotoxic stress tolerance in Arabidopsis. Plant Physiol. **145:** 843–852.

Kobayashi, Y., Kobayashi, Y., Sugimoto, M., Lakshmanan, V., Iuchi, S., Kobayashi, M., Bais, H.P., and Koyama, H. (2013). Characterization of the complex regulation of *AtALMT1* expression in response to phytohormones and other inducers. Plant Physiol. **162:** 732–740.

Kochian, L.V., Hoekenga, O.A., and Pineros, M.A. (2004). How do crop plants tolerate acid soils? Mechanisms of aluminum tolerance and phosphorous efficiency. Annu. Rev. Plant Biol. **55:** 459–493.

Kollmeier, M., Felle, H.H., and Horst, W.J. (2000). Genotypical differences in aluminum resistance of maize are expressed in the distal part of the transition zone. Is reduced basipetal auxin flow involved in inhibition of root elongation by aluminum? Plant Physiol. **122:** 945–956.

Kumari, M., Taylor, G.J., and Deyholos, M.K. (2008). Transcriptomic responses to aluminum stress in roots of *Arabidopsis thaliana*. Mol. Genet. Genomics **279:** 339–357.

Lavenus, J., Goh, T., Roberts, I., Guyomarc'h, S., Lucas, M., De Smet, I., Fukaki, H., Beeckman, T., Bennett, M., and Laplaze, L. (2013). Lateral root development in *Arabidopsis*: Fifty shades of auxin. Trends Plant Sci. **18:** 450–458.

Li, R., Yu, C., Li, Y., Lam, T.W., Yiu, S.M., Kristiansen, K., and Wang, J. (2009). SOAP2: An improved ultrafast tool for short read alignment. Bioinformatics **25:** 1966–1967.

Liu, J., Magalhaes, J.V., Shaff, J., and Kochian, L.V. (2009). Aluminum-activated citrate and malate transporters from the MATE and ALMT families function independently to confer *Arabidopsis* aluminum tolerance. Plant J. **57:** 389–399.

Liu, P.P., Montgomery, T.A., Fahlgren, N., Kasschau, K.D., Nonogaki, H., and Carrington, J.C. (2007). Repression of *AUXIN RESPONSE FACTOR10* by microRNA160 is critical for seed germination and post-germination stages. Plant J. **52:** 133–146.

Liu, X., Huang, J., Wang, Y., Khanna, K., Xie, Z., Owen, H.A., and Zhao, D. (2010). The role of floral organs in carpels, an Arabidopsis loss-of-function mutation in microRNA160a, in organogenesis and the mechanism regulating its expression. Plant J. **62:** 416–428.

Ma, J.F., Shen, R., Nagao, S., and Tanimoto, E. (2004). Aluminum targets elongating cells by reducing cell wall extensibility in wheat roots. Plant Cell Physiol. **45:** 583–589.

Mai, Y.X., Wang, L., and Yang, H.Q. (2011). A gain-of-function mutation in IAA7/AXR2 confers late flowering under short-day light in *Arabidopsis*. J. Integr. Plant Biol. **53:** 480–492.

Maron, L.G., Kirst, M., Mao, C., Milner, M.J., Menossi, M., and Kochian, L.V. (2008). Transcriptional profiling of aluminum toxicity and tolerance responses in maize roots. New Phytol. **179:** 116–128.

Massot, N., Nicander, B., Barceló, J., Poschenrieder, C., and Tillberg, E. (2002). A rapid increase in cytokinin levels and enhanced ethylene evolution precede Al^{3+}-induced inhibition of root growth in bean seedlings (*Phaseolus vulgaris* L.). Plant Growth Regul. **37:** 105–112.

Moore, A., Donahue, C.J., Bauer, K.D., and Mather, J.P. (1998). Simultaneous measurement of cell cycle and apoptotic cell death. Methods Cell Biol. **57:** 265–278.

Mortazavi, A., Williams, B.A., McCue, K., Schaeffer, L., and Wold, B. (2008). Mapping and quantifying mammalian transcriptomes by RNA-Seq. Nat. Methods **5:** 621–628.

Muday, G.K., Rahman, A., and Binder, B.M. (2012). Auxin and ethylene: Collaborators or competitors? Trends Plant Sci. **17:** 181–195.

Nishimura, T., Nakano, H., Hayashi, K., Niwa, C., and Koshiba, T. (2009). Differential downward stream of auxin synthesized at the tip has a key role in gravitropic curvature via TIR1/AFBs-mediated auxin signaling pathways. Plant Cell Physiol. **50:** 1874–1885.

Okushima, Y., Fukaki, H., Onoda, M., Theologis, A., and Tasaka, M. (2007). *ARF7* and *ARF19* regulate lateral root formation via direct activation of *LBD/ASL* genes in *Arabidopsis*. Plant Cell **19:** 118–130.

Overvoorde, P., Fukaki, H., and Beeckman, T. (2010). Auxin control of root development. Cold Spring Harb. Perspect. Biol. **2:** a001537.

Pan, W., Shou, S., Zhou, X., Guo, T., Zhu, M., and Pan, J. (2011). Al-induced cell wall hydroxyproline-rich glycoprotein accumulation is involved in alleviating Al toxicity in rice. Acta Physiol. Plant. **33:** 601–608.

Pickett, F.B., Wilson, A.K., and Estelle, M. (1990). The *aux1* mutation of Arabidopsis confers both auxin and ethylene resistance. Plant Physiol. **94:** 1462–1466.

Rademacher, E.H., Möller, B., Lokerse, A.S., Llavata-Peris, C.I., van den Berg, W., and Weijers, D. (2011). A cellular expression map of the Arabidopsis *AUXIN RESPONSE FACTOR* gene family. Plant J. **68:** 597–606.

Rangel, A.F., Rao, I.M., and Horst, W.J. (2007). Spatial aluminium sensitivity of root apices of two common bean (*Phaseolus vulgaris* L.) genotypes with contrasting aluminium resistance. J. Exp. Bot. **58:** 3895–3904.

Rosquete, M.R., von Wangenheim, D., Marhavý, P., Barbez, E., Stelzer, E.H., Benková, E., Maizel, A., and Kleine-Vehn, J. (2013). An auxin transport mechanism restricts positive orthogravitropism in lateral roots. Curr. Biol. **23:** 817–822.

Růzicka, K., Ljung, K., Vanneste, S., Podhorská, R., Beeckman, T., Friml, J., and Benková, E. (2007). Ethylene regulates root growth through effects on auxin biosynthesis and transport-dependent auxin distribution. Plant Cell **19:** 2197–2212.

Ryan, P.R., and Kochian, L.V. (1993). Interaction between aluminum toxicity and calcium uptake at the root apex in near-isogenic lines of wheat (*Triticum aestivum* L.) differing in aluminum tolerance. Plant Physiol. **102:** 975–982.

Ryan, P.R., Ditomaso, J.M., and Kochian, L.V. (1993). Aluminum toxicity in roots: An investigation of spatial sensitivity and the role of the root cap. J. Exp. Bot. **44:** 437–446.

Schlicht, M., Strnad, M., Scanlon, M.J., Mancuso, S., Hochholdinger, F., Palme, K., Volkmann, D., Menzel, D., and Baluška, F. (2006). Auxin immunolocalization implicates vesicular neurotransmitter-like mode of polar auxin transport in root apices. Plant Signal. Behav. **1:** 122–133.

Sivaguru, M., and Horst, W.J. (1998). The distal part of the transition zone is the most aluminum-sensitive apical root zone of maize. Plant Physiol. **116:** 155–163.

Sivaguru, M., Baluška, F., Volkmann, D., Felle, H.H., and Horst, W.J. (1999). Impacts of aluminum on the cytoskeleton of the maize root apex. Short-term effects on the distal part of the transition zone. Plant Physiol. **119:** 1073–1082.

Sivaguru, M., Liu, J., and Kochian, L.V. (2013). Targeted expression of *SbMATE* in the root distal transition zone is responsible for sorghum aluminum resistance. Plant J. **76:** 297–307.

Stepanova, A.N., Robertson-Hoyt, J., Yun, J., Benavente, L.M., Xie, D.Y., Doležal, K., Schlereth, A., Jürgens, G., and Alonso, J.M. (2008). TAA1-mediated auxin biosynthesis is essential for hormone crosstalk and plant development. Cell **133:** 177–191.

Stepanova, A.N., Yun, J., Likhacheva, A.V., and Alonso, J.M. (2007). Multilevel interactions between ethylene and auxin in *Arabidopsis* roots. Plant Cell **19:** 2169–2185.

Stepanova, A.N., Yun, J., Robles, L.M., Novak, O., He, W., Guo, H., Ljung, K., and Alonso, J.M. (2011). The *Arabidopsis* YUCCA1 flavin monooxygenase functions in the indole-3-pyruvic acid branch of auxin biosynthesis. Plant Cell **23:** 3961–3973.

Steward, N., Martin, R., Engasser, J.M., and Goergen, J.L. (1999). A new methodology for plant cell viability assessment using intracellular esterase activity. Plant Cell Rep. **19:** 171–176.

Sun, P., Tian, Q.Y., Chen, J., and Zhang, W.H. (2010). Aluminium-induced inhibition of root elongation in *Arabidopsis* is mediated by ethylene and auxin. J. Exp. Bot. **61:** 347–356.

Sun, P., Tian, Q.Y., Zhao, M.G., Dai, X.Y., Huang, J.H., Li, L.H., and Zhang, W.H. (2007). Aluminum-induced ethylene production is associated with inhibition of root elongation in *Lotus japonicus* L. Plant Cell Physiol. **48:** 1229–1235.

Swarup, R., Perry, P., Hagenbeek, D., Van Der Straeten, D., Beemster, G.T., Sandberg, G., Bhalerao, R., Ljung, K., and Bennett, M.J. (2007). Ethylene upregulates auxin biosynthesis in *Arabidopsis* seedlings to enhance inhibition of root cell elongation. Plant Cell **19:** 2186–2196.

Tabuchi, A., and Matsumoto, H. (2001). Changes in cell-wall properties of wheat (*Triticum aestivum*) roots during aluminum-induced growth inhibition. Physiol. Plant. **112:** 353–358.

Tao, Y., et al. (2008). Rapid synthesis of auxin via a new tryptophan-dependent pathway is required for shade avoidance in plants. Cell **133:** 164–176.

Teale, W.D., Paponov, I.A., Ditengou, F., and Palme, K. (2005). Auxin and the developing root of *Arabidopsis thaliana*. Physiol. Plant. **123:** 130–138.

Teale, W.D., Paponov, I.A., and Palme, K. (2006). Auxin in action: Signalling, transport and the control of plant growth and development. Nat. Rev. Mol. Cell Biol. **7:** 847–859.

Tian, H., Niu, T., Yu, Q., Quan, T., and Ding, Z. (2013). Auxin gradient is crucial for the maintenance of root distal stem cell identity in *Arabidopsis*. Plant Signal. Behav. **8:** e26429.

Tian, H., Wabnik, K., Niu, T., Li, H., Yu, Q., Pollmann, S., Vanneste, S., Govaerts, W., Rolcík, J., Geisler, M., Friml, J., and Ding, Z. (2014a). WOX5-IAA17 feedback circuit-mediated cellular auxin response is crucial for the patterning of root stem cell niches in *Arabidopsis*. Mol. Plant **7:** 277–289.

Tian, Q., Zhang, X., Ramesh, S., Gilliham, M., Tyerman, S.D., and Zhang, W.H. (2014b). Ethylene negatively regulates aluminium-induced malate efflux from wheat roots and tobacco cells transformed with *TaALMT1*. J. Exp. Bot. **65:** 2415–2426.

Tsutsui, T., Yamaji, N., Huang, C.F., Motoyama, R., Nagamura, Y., and Ma, J.F. (2012). Comparative genome-wide transcriptional analysis of Al-responsive genes reveals novel Al tolerance mechanisms in rice. PLoS ONE **7:** e48197–e48205.

Vanneste, S., et al. (2005). Cell cycle progression in the pericycle is not sufficient for SOLITARY ROOT/IAA14-mediated lateral root initiation in *Arabidopsis thaliana*. Plant Cell **17:** 3035–3050.

Verbelen, J.P., De Cnodder, T., Le, J., Vissenberg, K., and Baluška, F. (2006). The root apex of *Arabidopsis thaliana* consists of four distinct zones of growth activities: Meristematic zone, transition zone, fast elongation zone and growth terminating zone. Plant Signal. Behav. **1:** 296–304.

Von Uexküll, H.R., and Mutert, E. (1995). Global extent, development and economic impact of acid soils. Plant Soil **171:** 1–15.

Wang, J.W., Wang, L.J., Mao, Y.B., Cai, W.J., Xue, H.W., and Chen, X.Y. (2005). Control of root cap formation by microRNA-targeted auxin response factors in *Arabidopsis*. Plant Cell **17:** 2204–2216.

Yang, J.L., Zhu, X.F., Peng, Y.X., Zheng, C., Li, G.X., Liu, Y., Shi, Y.Z., and Zheng, S.J. (2011a). Cell wall hemicellulose contributes significantly to aluminum adsorption and root growth in *Arabidopsis*. Plant Physiol. **155:** 1885–1892.

Yang, Z.B., Eticha, D., Albacete, A., Rao, I.M., Roitsch, T., and Horst, W.J. (2012). Physiological and molecular analysis of the interaction between aluminium toxicity and drought stress in common bean (*Phaseolus vulgaris*). J. Exp. Bot. **63:** 3109–3125.

Yang, Z.B., Eticha, D., Rotter, B., Rao, I.M., and Horst, W.J. (2011b). Physiological and molecular analysis of polyethylene glycol-induced reduction of aluminium accumulation in the root tips of common bean (*Phaseolus vulgaris*). New Phytol. **192:** 99–113.

Yang, Z.B., Rao, I.M., and Horst, W.J. (2013). Interaction of aluminium and drought stress on root growth and crop yield on acid soils. Plant Soil **372:** 3–25.

Zeng, Q.Y., Yang, C.Y., Ma, Q.B., Li, X.P., Dong, W.W., and Nian, H. (2012). Identification of wild soybean miRNAs and their target genes responsive to aluminum stress. BMC Plant Biol. **12:** 182.

Zhao, Y., Christensen, S.K., Fankhauser, C., Cashman, J.R., Cohen, J.D., Weigel, D., and Chory, J. (2001). A role for flavin monooxygenase-like enzymes in auxin biosynthesis. Science **291:** 306–309.

Zhou, W., Wei, L., Xu, J., Zhai, Q., Jiang, H., Chen, R., Chen, Q., Sun, J., Chu, J., Zhu, L., Liu, C.M., and Li, C. (2010). *Arabidopsis* tyrosylprotein sulfotransferase acts in the auxin/PLETHORA pathway in regulating postembryonic maintenance of the root stem cell niche. Plant Cell **22:** 3692–3709.

Zhu, X.F., Lei, G.J., Wang, Z.W., Shi, Y.Z., Braam, J., Li, G.X., and Zheng, S.J. (2013). Coordination between apoplastic and symplastic detoxification confers plant aluminum resistance. Plant Physiol. **162:** 1947–1955.

Zhu, X.F., et al. (2012). *XTH31*, encoding an in vitro XEH/XET-active enzyme, regulates aluminum sensitivity by modulating in vivo XET action, cell wall xyloglucan content, and aluminum binding capacity in *Arabidopsis*. Plant Cell **24:** 4731–4747.